

Conjugates of Antisense Oligonucleotides with the Tat and Antennapedia Cell-Penetrating Peptides: Effects on Cellular Uptake, Binding to Target Sequences, and Biologic Actions

Anna Astriab-Fisher,¹ Dimitri Sergueev,² Michael Fisher,¹ Barbara Ramsay Shaw,² and R. L. Juliano^{1,3}

Received February 19, 2002; accepted February 28, 2002

Purpose. The attainment of effective intracellular delivery remains an important issue for pharmacologic applications of antisense oligonucleotides. Here, we describe the synthesis, binding properties, and biologic properties of peptide-oligonucleotide conjugates comprised of the Tat and Ant cell-penetrating peptides with 2'-*O*-methyl phosphorothioate oligonucleotides.

Methods. The biologic assay used in this study measures the ability of the antisense molecule to correct splicing of an aberrant intron inserted into the Luciferase gene; thus, this assay clearly demonstrates the delivery of functional antisense molecules to the splicing machinery within the nucleus. The binding affinities of the conjugates to their target sequences were measured by surface plasmon resonance (BIAcor) techniques.

Results. The peptide-oligonucleotide conjugates progressively entered cells over a period of hours and were detected in cytoplasmic vesicles and in the nucleus. Peptide-oligonucleotide conjugates targeted to the aberrant splice site, but not mismatched controls, caused an increase in Luciferase activity in a dose-responsive manner. The kinetics of Luciferase appearance were consistent with the course of the uptake process for the conjugates. The effects of peptide conjugation on the hybridization characteristics of the oligonucleotides were also examined using surface plasmon resonance. The peptide-oligonucleotide conjugates displayed binding affinities and selectivities similar to those of unconjugated oligonucleotides.

Conclusions. Conjugation with cell-penetrating peptides enhances oligonucleotide delivery to the nucleus without interfering with the base-pairing function of antisense oligonucleotides.

KEY WORDS: antisense; oligonucleotide; delivery; peptide; conjugate.

INTRODUCTION

Antisense oligonucleotides potentially have the ability to inhibit the expression of virtually any gene. Thus, antisense technology has attracted considerable interest as a possible therapeutic approach (1–3), and several antisense molecules have already reached phase I or II clinical trials (4–6). However, one of the major obstacles to effective use of oligonucleotides as therapeutic agents is their relatively poor entry into cells (7,8). Thus, a great deal of effort has gone into devising means for enhancing the intracellular delivery of oligonucleotides. Although cationic lipids (9,10) and polymer carriers (11,12) have been widely used in the laboratory setting, a new approach involving conjugation of oligonucleotides to “cell-penetrating peptides” seems particularly promising (13). Peptide-oligonucleotide conjugates, unlike oligonucleotide complexes with cationic lipids or polymers, are of relatively modest molecular size. Thus, they are more likely to evade uptake by the phagocytes of the reticuloendothelial system and to attain a widespread biodistribution subsequent to *in vivo* administration (14), similar to the case of unmodified oligonucleotides.

Recent work has demonstrated that certain peptide sequences can facilitate the entry of other peptides, oligonucleotides, and even proteins into the cytoplasm of cells. Two examples of such cell-penetrating peptides are a 35-amino acid basic sequence (Tat) from the HIV Tat protein (15) and a 16-amino acid basic sequence (Ant) from the *Drosophila* antennapedia protein (16). A more compact version of the Tat sequence is also functional (17). Antennapedia-type peptides have been used to deliver oligonucleotides, including peptide-nucleic acids, into cells (18,19). Furthermore, our group has successfully used both Tat and Ant conjugates of phosphorothioate antisense oligonucleotides to regulate the expression of MDR1, a gene associated with drug resistance in cancer cells (20). The powerful capabilities of cell-penetrating peptides such as Tat are attested to by their successful use in promoting the intracellular delivery of large proteins (13,21,22). Thus, in terms of antisense pharmacology, it seems important to understand more fully the effects of cell-penetrating peptides in terms of intracellular delivery of oligonucleotides, interactions with target nucleic acids, and pharmacologic actions.

One of the problems with conventional approaches to the evaluation of antisense molecules is that the biologic effect usually attained by antisense is an inhibition of gene expression. Thus, it is easy to confuse non-specific toxic effects with bonafide antisense actions. To remedy this problem, a new approach for evaluating antisense actions has been developed. This approach is based on the observation that certain types of oligonucleotides (those that do not support RNase H activity) can alter RNA splice site selection (23–25). This information has been used to devise a sensitive and accurate new assay that provides a positive readout of antisense action. Thus, an aberrant intron from thalassemic beta-globin is inserted into the coding sequence of the Luciferase reporter gene. The intron cannot be properly spliced out and results in the presence of an in frame stop codon in the message, thus preventing Luciferase expression. However, the presence of an antisense oligonucleotide complementary to the aberrant splice site will allow correct splicing and the subsequent expression of functional Luciferase (26). This is an excellent system for evaluating the delivery of oligonucleotides because only the appearance of a specific oligonucleotide within the nucleus of a viable cell will allow correct splicing and consequent Luciferase expression; therefore, there can be no confusion between antisense effects and cytotoxic effects.

¹ Department of Pharmacology, School of Medicine, University of North Carolina, Chapel Hill, North Carolina 27599.

² Department of Chemistry, Duke University, Durham, North Carolina 27708.

³ To whom correspondence should be addressed. (arjay@med.unc.edu)

We have used the splicing correction assay to evaluate the pharmacologic potential of antisense oligonucleotides chemically coupled to versions of the Tat and Ant cell-penetrating peptides. The oligonucleotides used were 2'-*O*-methyl-phosphorothioates, which do not support RNase H and thus can be used for this type of assay. In these studies, we have examined cellular uptake and subcellular compartmentation of the peptide-oligonucleotide conjugates by flow cytometry and fluorescence microscopy. We have also used surface plasmon resonance measurements to evaluate whether the presence of the conjugated peptide affects the ability of the oligonucleotide to interact with its nucleic acid target. Finally, we tested the biologic activity of the peptide-oligonucleotide conjugates using the splicing correction assay. These studies provide new insights into the possibilities and limitations of antisense oligonucleotide conjugates with cell-penetrating peptides.

METHODS

Synthesis of Peptide-Oligonucleotide Conjugates

Peptides

NH₂-RKKRRQRRRPPQC-COOH (Tat) and NH₂-RQIKIWFQNRRMKWKKGGC-COOH (Ant) were synthesized by the Protein Chemistry Core facility, Department of Chemistry, University of North Carolina (Chapel Hill, North Carolina).

Synthesis of Oligonucleotides Bearing 3'-NH₂ and 5'-SH Groups

Solid-phase syntheses of the oligonucleotide (2'-*O*-methylribonucleoside) antisense phosphorothioate HS-(CH₂)₆-5'-O-CCU-CUU-ACC-UCA-GUU-ACA-3'-*O*-CH₂CH(CH₂OH)(CH₂)₄NH₂ (**1**) and an analogous compound with 5 mismatches, 5'-CCU-AUU-UCC-ACA-CUU-UCA-3' (**2**), were performed at a 10- μ mole scale on a 392 ABI DNA synthesizer. 3'-amino-modifier C7 CPG (Glen Research) was used as the solid support to introduce a 3'-NH₂ group, and the last coupling was performed with thiol-modifier C6 S-S (Glen Research) to generate a 5'-SH group after deprotection. Standard 10- μ mole phosphoramidite cycles were used except that the coupling time was increased to 6 min and sulfurization with Beaucage's reagent was carried out for 5 min. The oligonucleotides were cleaved from the solid support and deprotected by treatment with concentrated ammonia containing 50 mM dithiothreitol (DTT; Sigma Chemical Co., St. Louis, Missouri) for 8 h at 5°C.

Synthesis of 5'-(2-Thiopyridyl) Oligonucleotide Derivatives

The deprotection reaction mixtures were evaporated to dryness and resuspended in 3 mL of 0.1 M KH₂PO₄ (pH 7.5) buffer. Residual DTT was removed by extraction with ethylacetate:n-butanol (3:1) (4 mL, 3 times), after which 44 mg (0.2 mmol) of 2,2'-dithiodipyridine (Aldrich) was added under argon. After overnight incubation, the 5'-(2-thiopyridyl) derivatives of the oligonucleotides (**PyS-1**, **PyS-2**) were isolated by IE high-performance liquid chromatography (HPLC) on a Mono Q (10 \times 100 mm) column (Pharmacia) using a 0.0–1.2 M gradient of KBr over 60 min in 70 mM KH₂PO₄ (pH 6.5), 30% CH₃CN and were further purified by reverse-phase

(RP) HPLC. The presence of the 5'-PyS group was confirmed by reduction with 2-mercaptoethanol (50 mM, 100 eq., 10 min) and spectrophotometric detection of the resulting PySH at 343 nm. Yields were 30% (i.e. 3.0 μ moles) for both **PyS-1** and **PyS-2**.

3' Fluorescent Labeling

The 5'-PyS-3'-NH₂ oligonucleotides (3.0 μ mole) were dissolved in 0.9 mL of 0.2 M Na₂CO₃/NaHCO₃ (pH 9.0) buffer and 90 μ L of 0.2 M 5-(and-6)-carboxytetramethylrhodamine *N*-hydroxysuccinimidyl ester (NHS-TAMRA, Molecular Probes) (18 μ mole, 6 eq.) in DMSO was added. The reaction mixture was incubated in the dark at 37°C for 4 h and excess dye was removed by gel-filtration on a Spherilose GCL-25 (Isco, Inc.) (10 \times 250 mm) column.

Conjugation of Fluorescently Labeled PyS-1(2) with Peptides

Oligonucleotide (1.5 μ mole) was dissolved in 1.5 mL of 0.1 M KH₂PO₄ (pH 7.5), 0.3 M KBr, 8 M urea buffer. The solution was degassed and 5.7 mg of Tat (3.2 μ mole, 2.1 eq.) or 16.1 mg of Ant (6.5 μ mole, 4.3 eq.) was added under argon. The reaction mixtures were incubated overnight under argon at r.t. The resulting conjugates were separated by IE HPLC on a Mono Q (10 \times 100 mm) column using a 0–1.2 M gradient of KBr established over 60 min in 70 mM KH₂PO₄ (pH 6.5), 5 M urea, 30% CH₃CN. Yields: **Tat-1** (81%), **Tat-2** (85%), **Ant-1** (40%), **Ant-2** (50%). The amounts of the conjugates were determined spectrophotometrically based on the calculated molar absorption coefficients at $\lambda = 260$ nm for **Tat-1** ($\epsilon = 199,000$ M⁻¹cm⁻¹), **Ant-1** ($\epsilon = 213,000$ M⁻¹cm⁻¹), **Tat-2** ($\epsilon = 197,600$ M⁻¹cm⁻¹), and **Ant-2** ($\epsilon = 211,600$ M⁻¹cm⁻¹). RP HPLC and 20% denaturing PAGE analyses were used to check the purity of the conjugates and to verify the composition. For control experiments, the 3'-fluorescently labeled oligonucleotide **1** having the 5'-OH group (no peptide) was synthesized. The overall synthetic strategy was similar to one published by Vives and Lebleu (27). Note that in the sections below **Tat-1** is usually referred to as Tat-18 antisense, whereas **Tat-2** is termed Tat-18 mismatched control, similarly for the Ant conjugates.

Cells

Hela/705 cells were a gift from R Kole. These cells are stably transfected with a recombinant plasmid (pLuc/705) carrying the luciferase gene interrupted by a mutated human-beta globin intron 2 (IVS2-705). The mutation in the intron causes aberrant splicing of luciferase pre-mRNA, preventing translation of luciferase, unless corrected by the presence of an antisense oligonucleotide targeted to the splice site (26). The cells were grown in DMEM-H medium containing 10% fetal bovine serum (FBS) and in an atmosphere of 95% air, 5% CO₂.

Treatment of Cells with Peptide-Oligonucleotide Conjugates

The experimental protocols were similar to those previously described (20). Briefly, Hela-705 cells were grown in 162 mm flasks to 95% confluency and then seeded into 100 mm dishes at a concentration of 5 \times 10⁶/dish in 10% FBS/

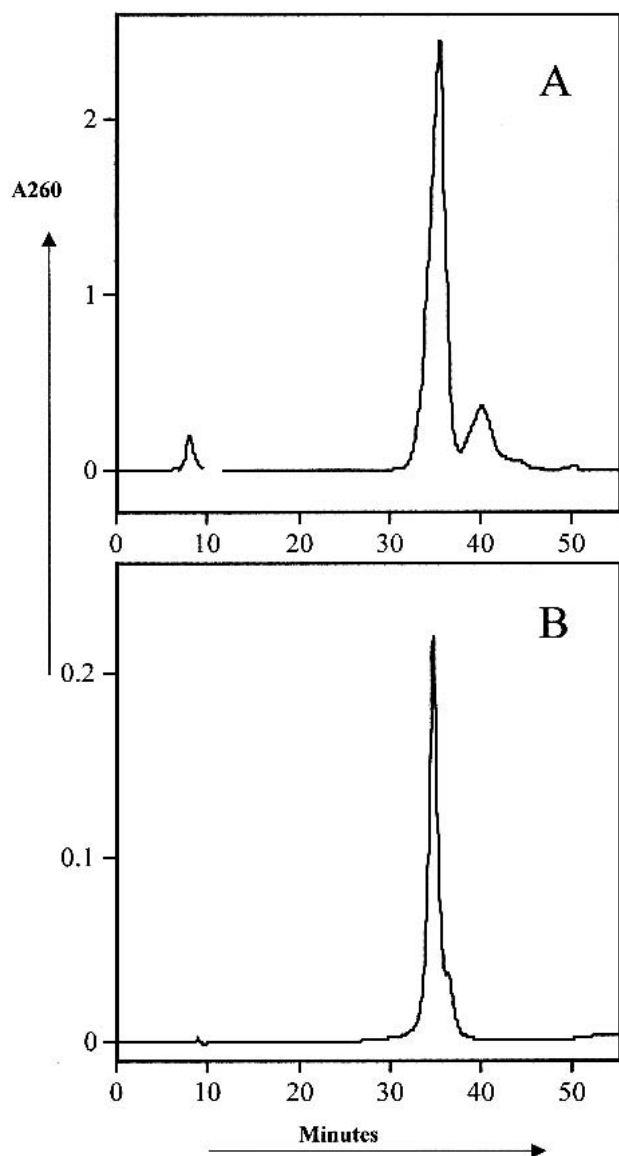


Fig. 1. IE HPLC isolation (A) and subsequent analysis (B) of the Tat-18 peptide-oligonucleotide conjugate. Abcissa, time of elution; ordinate, absorbance at 260 nm.

DMEM-H and incubated for 24 h. The cells were washed twice with phosphate-buffered saline (PBS). Peptide-oligonucleotide conjugates, free oligonucleotide, or oligonucleotide complexed with Lipofectin® (20 µg/mL) were mixed in Opti-MEM and incubated with cells at 37°C, usually for 6 h. The concentrations for all oligonucleotides and conjugates were between 0.05–1 µM.

Uptake and Cellular Distribution of Peptide-Oligonucleotide Conjugates

After treatment with peptide-oligonucleotide conjugates, oligonucleotides, or oligonucleotides with Lipofectin, the cells were removed with trypsin/EDTA and split for fluorescence microscopy or flow cytometry analysis. Half of the cells were resuspended in 1 mL 10% FBS/DMEM and incubated for 6 h on fibronectin (10 µg/mL)-coated cover slides. The distribution of fluorescence was analyzed on a Zeiss Axiophot

equipped for transmitted light and incident-light fluorescence analysis, with a 100-watt mercury lamp, oil immersion objective (FLUAR 40X/1.30 Oil/0.17), and an H5546 filter. Images were captured with a slow scan charge-coupled device Video Camera System (Carl Zeiss, Inc. ZVSTM3C75DE) using the MetaMorph Imaging System (Version 3.5, Universal Imaging Corporation). For flow cytometry analysis, the cells were resuspended in 500 µL of PBS and measured for the accumulation of TAMRA marker on a Becton Dickinson flow cytometer and analyzed using Cicero software.

Biological Effects of Peptide-Oligonucleotide Treatment

To detect Luciferase expression, the LucLite Luciferase Reporter Gene Assay (Packard) and TopCount® NXT™ Microplate Scintillation and Luminescence Counter were used. The cells were incubated with peptide-oligonucleotide conjugates for periods between 6–48 h in different experiments, in the presence or absence of serum, and subsequently the medium was replaced with 10% FBS/DMEM. An additional 5–35 h later, the cells were rinsed with PBS, trypsinized and split. Half of the cells were counted on an ElectroZone cellscope (Particle Data, Inc., Elmhurst, Illinois) for normalization, the other half were resuspended in 100 µL of phenol red free DMEM-H and transferred to a 96-well luminescence plate. Reconstituted substrate in a volume of 100 µL was added to each well containing the cells in culture medium. The plates were sealed and, to reduce microplate phosphorescence, the plates were dark adapted for ten minutes before counting on the TopCount®. Measurement of luminescence was performed at 22°C in single photon-counting luminescence mode.

Dissociation and Association Constant Analysis

Biomolecular interaction analysis (28) was performed using the BIAcore 2000 (Pharmacia) with SA Sensor chips (Pharmacia) containing streptavidin chemically coupled to a dextran matrix. All kinetic experiments were performed in HBS buffer (150 mM NaCl containing 0.1 mM EDTA and 20 mM sodium phosphate adjusted to pH 7.0). The experiments were performed at 20°C for all systems. To reduce the diffusion distance and improve reference subtraction, the samples were injected at a high (20 µL/min) flow rate. To perform the

Table I.

Name	Sequence
Ant-18	NH2RQIKIWFQNRMRKWKGGC (COOH)S-S-5'-CCU-CUU-ACC-UCA-GUU-ACA-3'-NH2-TAMRA
Ant 18 mismatch	NH2RQIKIWFQNRMRKWKGGC COOHSS-5'CUU-AUU-UCC ACA-CUU-UCA-3'-NH2-TAMRA
Tat-18	NH2RKKRRRQRRPPQC(COOH)-S-S-5'- CCU-CUU-ACC-UCA-GUU-ACA- 3'-NH-TAMRA
Tat 18 mismatch	NH2RKKRRRQRRRPPQC(COOH)-S-S-5' CUU-AUU-UCCACA-CUU-UCA- 3'-NH-TAMRA
18-OH	5' CCU-CUU-ACC-UCA-GUU-ACA- 3'-NH-TAMRA

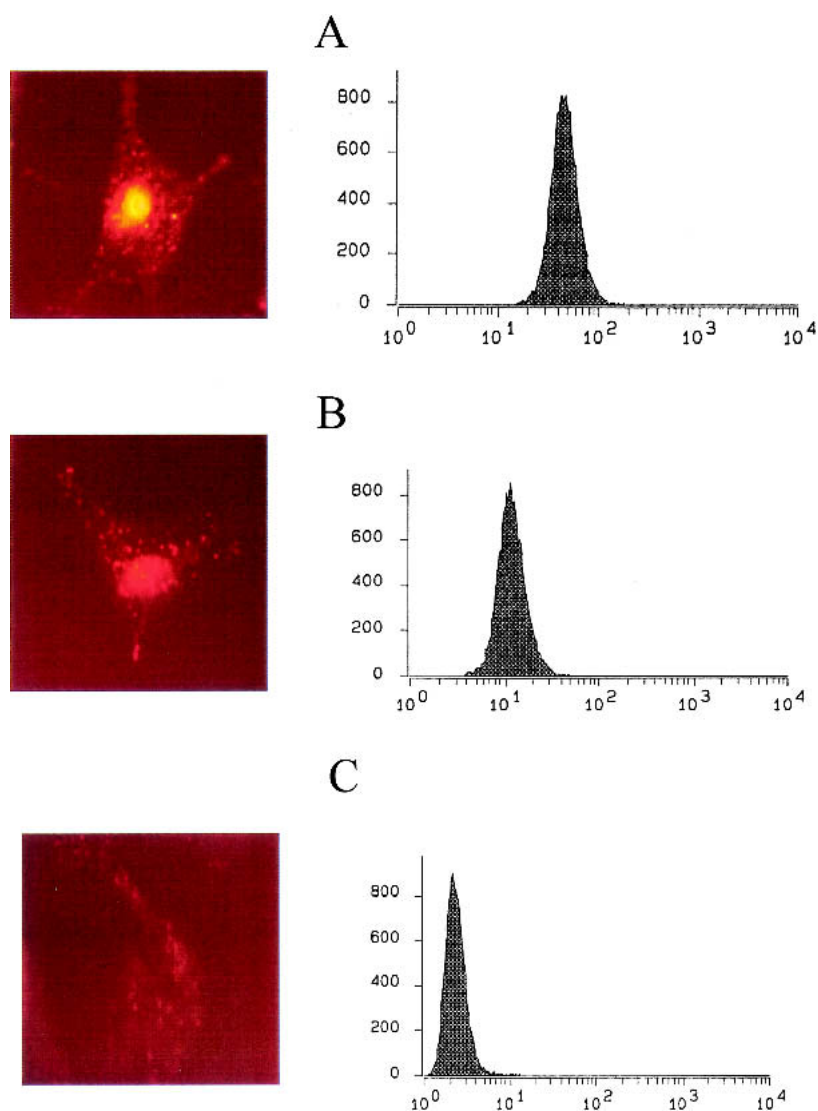


Fig. 2. Cellular uptake of peptide-oligonucleotide conjugates into HeLa 705 cells. Left panels: fluorescence microscopy using a Zeiss Axioscop with 40X oil objective. Right panels: flow cytometry: ordinate, number of cells; abscissa, fluorescence intensity. (A) oligonucleotide 18 transfected using Lipofectin (20 $\mu\text{g}/\text{mL}$) as a positive control. (B) peptide-oligonucleotide conjugate, Tat-18. (C) oligonucleotide 18 with no delivery agent as a negative control. The concentration of oligonucleotide 18 in A, B, and C was 0.5 μM , and the incubation time at 37°C was 4 h.

BIAcore analysis, first the 5' biotinylated oligonucleotides were immobilized on the streptavidin-coated surface of the sensor chip. Several different sequences including BIA 18 (18mer sequence complementary the peptide-oligonucleotide conjugates) and an 18-mer random oligonucleotide were used. Biotinylated oligonucleotides were dissolved in degassed HBS buffer at a concentration of 0.1 $\mu\text{g}/\text{mL}$ and injected (40 μL) over the streptavidin surface of the chip. Then the TAT-18, TAT-18 mismatch, and 18-OH oligonucleotides were injected (20 μL) over the reference and active chip surfaces at four different concentrations (10 $\mu\text{g}/\text{mL}$; 5 $\mu\text{g}/\text{mL}$; 2.5 $\mu\text{g}/\text{mL}$; and 1 $\mu\text{g}/\text{mL}$). Regeneration was performed between the reaction cycles (10 mM HCl; 10 μL). To avoid the possibility of carrying over the regeneration fluid between reaction and regeneration cycles, a series of blank injections and washing steps were run.

RESULTS

Synthesis of Peptide-Oligonucleotide Conjugates

One important issue in the use of oligonucleotides as therapeutic agents is their limited ability to cross cell membranes. Among the strategies to increase oligonucleotide penetration has been the covalent attachment of short cell penetrating peptides promising (13). For our studies, we chose 5'-end attachment of the peptides through a disulfide bond, which is readily formed and chemically stable, although potentially bio-reversible within the cell. We reserved the 3'-end to introduce a fluorescent reporter moiety via a primary amino group. Solid-phase syntheses of the oligonucleotides having 5'-SH and 3'-NH₂ functionalities, further activation of 5'-SH with 2-thiopyridyl group, and 3'-labeling with TAMRA

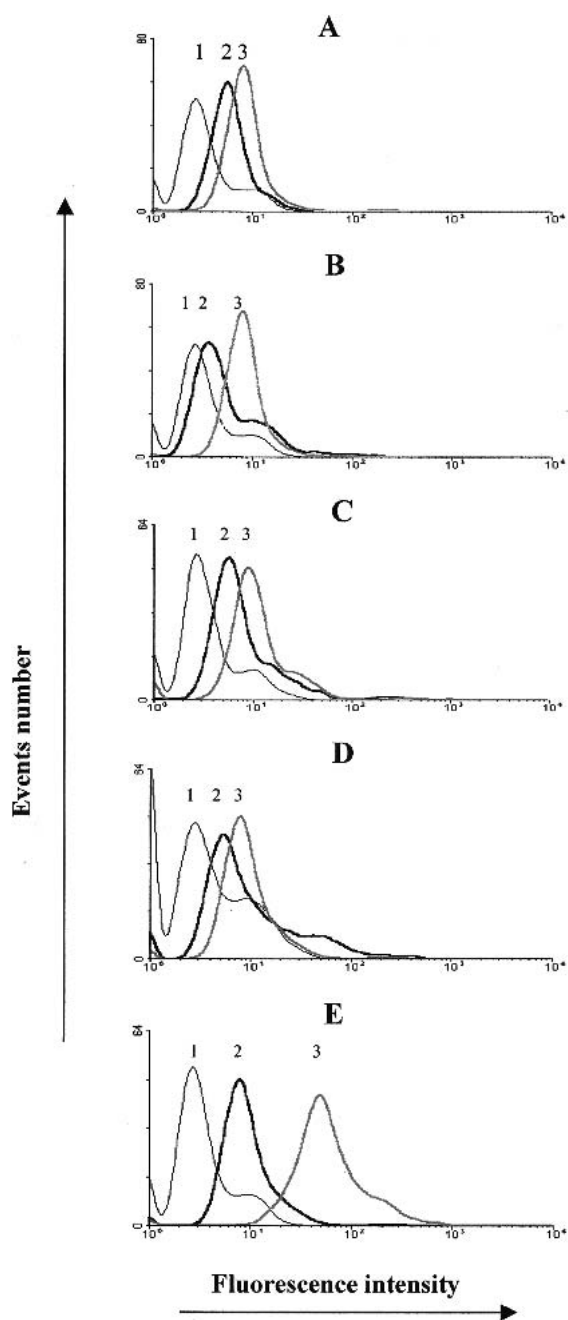


Fig. 3. Time dependence of cellular uptake of peptide-oligonucleotide conjugates. Analysis of uptake by HeLa 705 cells in the presence or absence of 10% FBS using flow cytometry: The concentration of conjugate was 0.5 μ M in all cases. The traces marked 1,2, 3 represent uptake after 30 min, 2 h, and 4 h, respectively. (A) Tat-18 in serum-free medium; (B) Tat-18 in 10% serum; (C) Ant-18 in serum-free medium; (D) Ant-18 in 10% serum; (E) oligonucleotide-18 complexed with Lipofectin in serum-free medium.

fluorophore all proceeded smoothly with high efficiency. The peptide conjugation reaction occurred through displacement of the 5'-PyS moiety of the oligonucleotide by the SH group of C-terminal cysteine. The conjugates were separated from the reaction mixture by anion-exchange (IE) HPLC (Fig.1a). Conjugation with the Tat peptide gave better yields (81% for Tat-1-TAMRA and 85% for Tat-2-TAMRA) than the reaction with the Ant peptide (40% for Ant-1-TAMRA and 50%

for Ant-2-TAMRA). The purity of the conjugates was checked by RP and IE HPLC (Fig.1b) and by 20% denaturing PAGE. Both methods demonstrated high purity for each of the prepared compounds (90–95% of the major component). Their characteristics, such as chromatographic retention times, UV/VIS spectra, and mobilities on 20% denaturing PAGE, were all consistent with the conjugate structures. In addition, treatment of the conjugates with a 50-fold excess of DTT produced the original oligonucleotides. Thus the synthetic scheme yielded the desired peptide-oligonucleotide conjugates. The sequences of the various conjugates are depicted in Table I.

Cellular Uptake and Subcellular Distribution of Peptide-Oligonucleotide Conjugates

The cellular uptake of oligonucleotides was examined as follows. HeLa 705 cells were treated for 4 h with TAMRA-labeled Tat 18 antisense conjugate with free TAMRA-labeled 18-mer oligonucleotide or with the same oligonucleotide complexed with commercial Lipofectin. Quantitation of total cellular uptake was done by flow cytometry, whereas the subcellular distribution of TAMRA-labeled oligonucleotide was visualized by digitized fluorescence microscopy. As seen in Figure 2, the use of Lipofectin provides the greatest total cellular accumulation of oligonucleotide, followed by the Tat peptide-oligonucleotide conjugate; there was virtually no uptake of free oligonucleotide. For both the peptide-oligonucleotide conjugate and for the oligonucleotide delivered by Lipofectin, fluorescence was visualized both in the nucleus and in cytoplasmic vesicles; the fluorescence microscopy images paralleled the flow cytometry data, with the greatest total nuclear fluorescence in the cells treated with Lipofectin. Similar observations were made using the Ant-peptide-oligonucleotide conjugate (data not shown). Thus, the Tat and Ant cell-penetrating peptides can promote the delivery of oligonucleotides to the cytoplasm and nucleus of cells in culture; however, they are not as effective as a cationic lipid preparation for the same concentration of oligonucleotide.

Kinetics of Cellular Uptake of Peptide-Oligonucleotide Conjugates

It has been reported elsewhere that cell-penetrating peptides such as Tat and Ant enter cells quickly (13,17). We thus wished to test how rapidly the peptide-oligonucleotide complexes were accumulated in cells; this was evaluated using TAMRA-labeled conjugates and flow cytometry. As seen in Figure 3, for both the Tat and Ant peptide-oligonucleotide conjugates, there was a progressive uptake over the period 30 min to 4 h; thereafter, the total cellular accumulation leveled off, suggesting that an equilibrium had been attained (data not shown). Furthermore, there was very little effect of serum on the rate or extent of accumulation. These observations suggest that the rate of intracellular accumulation of the peptide-oligonucleotide conjugates is considerably slower than that reported previously for the peptides alone (13). In addition, we observed a greater degree of localization within cytosolic vesicles than has been reported previously for free peptide. Thus, the presence of a rather large, highly anionic oligonucleotide moiety may retard the ability of the cell-

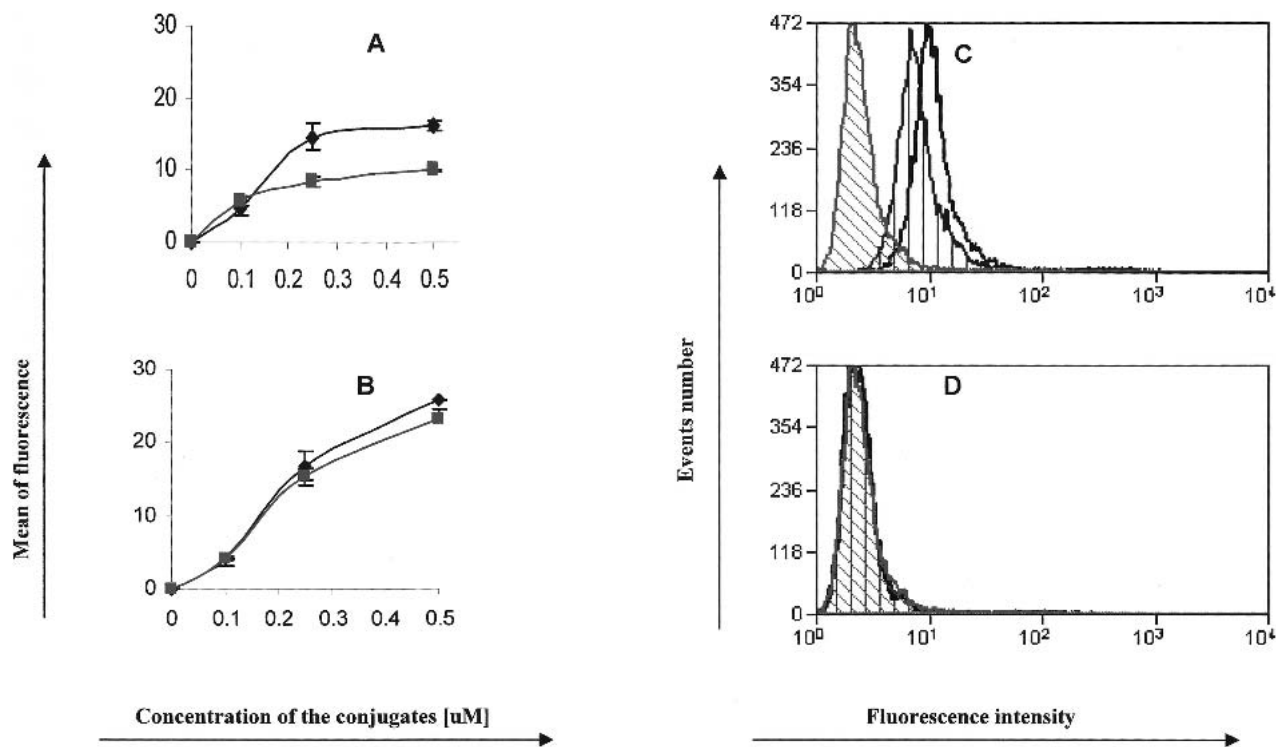


Fig. 4. Additional studies of peptide-oligonucleotide uptake. In (A) and (B), uptake of the conjugates was examined as a function of concentration during a 4-h interval in serum-containing medium. Solid triangles represent the Tat-18 conjugate whereas solid squares represent the Ant-18 conjugate. (A) HeLa cells growing attached to tissue culture dishes. (B) Jurkat cells growing in suspension culture. In (C) and (D), uptake was examined as a function of temperature. HeLa cells were exposed to oligo-18 (diagonal line shading), Ant-18 (vertical line shading), or Tat-18 (no shading) for 4 h at 37°C (C) or 4°C (D). Uptake was monitored by flow cytometry.

penetrating peptides to cross membranes and also affect the sub-cellular distribution. It should be noted that the measurements presented here define the total cellular accumulation of conjugate; they do not discriminate between material entering the cell by diffusion, uptake by endocytosis, or simple binding to the cell surface. However, surface adsorption is likely to be completed very quickly; thus, most of the accumulation reported here most probably represents material that has entered into several intracellular compartments.

To further investigate the uptake process for the conjugates, we examined another cell type. In Figure 4 (A and B), we compared uptake of the Tat and Ant peptide-oligonucleotide conjugates in substratum-attached HeLa cells and in Jurkat lymphoid cells in suspension. As seen in the figure, the total cellular accumulation of conjugates was similar in both cell types. Thus, both attached epithelial cells and suspension lymphoid cells can accumulate the conjugates, suggesting that many cell types will share this capability. We also examined the effect of temperature on the uptake process (Fig. 4, C and D). Somewhat surprisingly, we found that the cellular accumulation of conjugates was clearly temperature dependent, suggesting the involvement of an active internalization process. This contrasts with studies using the Tat or Ant delivery peptides alone, or conjugated to small peptides, where it has been shown that cellular accumulation occurs effectively at both 4°C and 37°C (13,17). Based on this observation and the fluorescent images of Figure 2, it seems likely that the peptide-oligonucleotide conjugates accumulate in endosomal compartments before entering the cytoplasm and nucleus, rather than directly penetrating across the

plasma membrane, as has been claimed for the unconjugated peptides.

Toxicity of Peptide-Oligonucleotide Conjugates

We evaluated the cytotoxicity of the peptide-oligonucleotide conjugates using a vital dye reduction assay. As seen in Figure 5, there was little effect of the Tat or Ant peptide-oligonucleotide conjugates on HeLa cell survival and growth in the concentration range used in our studies. Con-

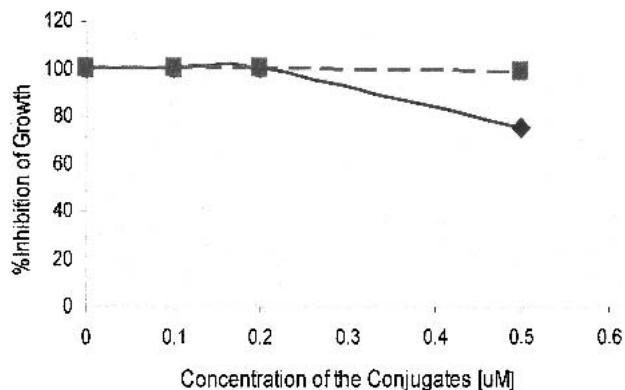


Fig. 5. Toxicity of peptide-oligonucleotide conjugates. HeLa 705 cells were treated with the indicated concentrations of Tat-18 (squares) or Ant-18 (diamonds) for 48 h in medium containing 10% serum. Thereafter, the number of viable cells was determined using the MTT assay. Mean for 4 determinations shown.

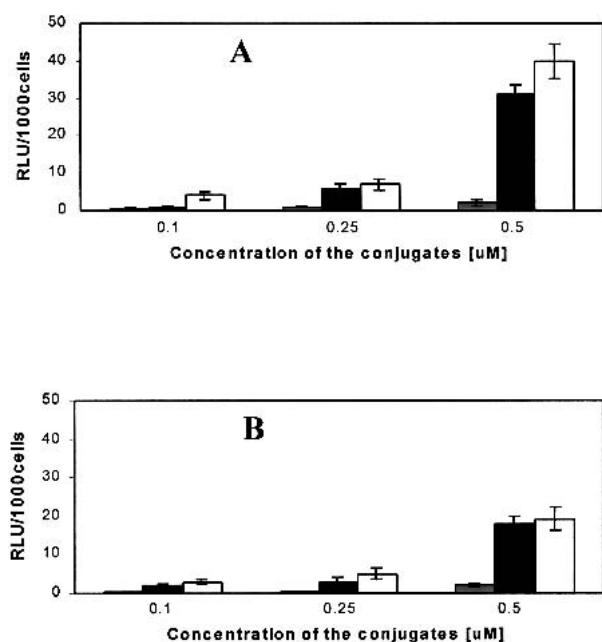


Fig. 6. Biologic effects of peptide-oligonucleotide conjugates. HeLa 705 cells were treated with various concentrations of peptide-oligonucleotide conjugates for 48 h in medium with or without 10% serum. At the end of the experimental period, cells were harvested, counted, and analyzed for Luciferase activity. The white bars represent cells treated with antisense conjugate in the presence of 10% serum. The black bars represent cells treated with antisense conjugate in serum-free medium. The gray bars represent cells treated with mismatch peptide-oligonucleotide conjugate in serum-free medium. (A) Tat-oligonucleotide conjugates. (B) Ant-oligonucleotide conjugates. Data represent the means and standard errors of three determinations. These experiments were repeated several times with similar results.

centrations in excess of 2 μM began to show significant toxicity (data not shown).

Pharmacologic Effects of Peptide-Oligonucleotide Conjugates

We used the Luciferase based splice correction assay described above to evaluate the ability of the peptide-oligonucleotide conjugates to produce biologic effects within cells. Thus, HeLa 705 were treated with various concentrations of Tat or Ant conjugates of antisense or mis-matched control oligonucleotides, for a period of 48 h in serum-free or serum-containing medium. In some cases, cells were treated with unconjugated antisense or mis-match control oligonucleotides. As seen in Figure 6, there was a progressive increase in Luciferase activity in cells treated with increasing concentrations of Tat- (Fig. 6A) or Ant- (Fig. 6B) peptide-antisense oligonucleotide conjugates. These effects were similar in cells maintained in serum-free or serum-replete conditions. Furthermore, there was very little effect of peptide conjugates made with the mismatched oligonucleotide, indicating that the observed effects are quite sequence selective. It should be noted that the maximal effects attained with the conjugates were several fold less than those attained with similar amounts of antisense oligonucleotide complexed with Lipofectin (data not shown); thus, the overall effect was approxi-

mately parallel to the total cellular accumulation of oligonucleotide.

We also evaluated the onset and duration of the antisense effects (Fig. 7A). Cells were exposed to peptide-oligonucleotide conjugates for a 6-h period in serum-free medium; thereafter, the medium was replaced with serum-containing medium, and Luciferase activity monitored periodically. As seen, Luciferase activity reached a peak at about 6 h. after exposure to serum and then gradually declined over the next 20+ h. In Fig. 7B, we examined the retention of the fluorophore-labeled conjugates in the cells. The data in Figure 7(A and B) indicate the following: 1) There is a delay of several hours between initial exposure to the conjugates and the accumulation of significant luciferase activity; this is to be expected because the splice correction process must occur and the new protein must be produced and 2) the rate of decline of luciferase activity is greater than the loss of the fluorophore derived from the conjugates. This suggests that the active (oligonucleotide) portion of the conjugate becomes relatively rapidly inactivated although the fluorophore label is only slowly lost from the cells.

Binding Studies Using Surface Plasmon Resonance

Because cationic peptides such as Tat and Ant might conceivably interact strongly with polyanionic nucleic acids, we wished to test whether the presence of the peptide influenced the binding affinity of the oligonucleotide for its target. In particular, we were concerned that the peptide might reduce the specificity of binding; however, this turned out not to be the case. The various conjugates or unconjugated oligonucleotides were reacted with a complementary sequence (BIA 18) or a "scrambled" sequence (Random 18) immobilized as biotin derivatives (see Table II) on a BIAcore sensor chip. Figure 8A represents typical surface plasmon resonance sensograms obtained for the Tat-18 conjugate, binding at different concentrations to its complementary immobilized oligonucleotide. As expected, the dissociation kinetics showed no significant dependence on concentration (according to: $[AB] = [AB]_0 e^{-k_d(t-t_0)}$ where $[AB]_0$ is the duplex concentration at time t_0 and k_d the dissociation rate constant), whereas the association rate increased with the concentration of the incoming strand A ($[AB] = k_a [A][B]_0 / (k_a [A] + k_d [1 - e^{-(k_a[A] + k_d)t}])$). As seen in Figure 8B, there was very little binding of the conjugate composed of Tat peptide coupled to a mis-match oligonucleotide sequence; thus there seems to be little effect on specificity. As seen in Figure 8C, the binding of Tat-18 conjugate to its complement is only slightly stronger than the binding of unmodified 18-mer oligonucleotide to the same target, indicating that base pairing is the predominant mode of interaction, rather than charge-dependent association between the cationic peptide and the anionic immobilized oligonucleotide.

Based on several experiments of this type, rate and equilibrium constants were calculated using BIAevaluation software 3.0, and are presented in Table III. As shown, the binding parameters for Tat-18 and for unconjugated 18-OH were very similar. A fluorescence microscope view of the sensor chip showing differential binding for fluorescent labeled Tat-18, oligonucleotide 18, and Tat-18 mismatch is presented in Figure 7D. It visually confirms the relative binding of the three types of molecules to the immobilized oligo-

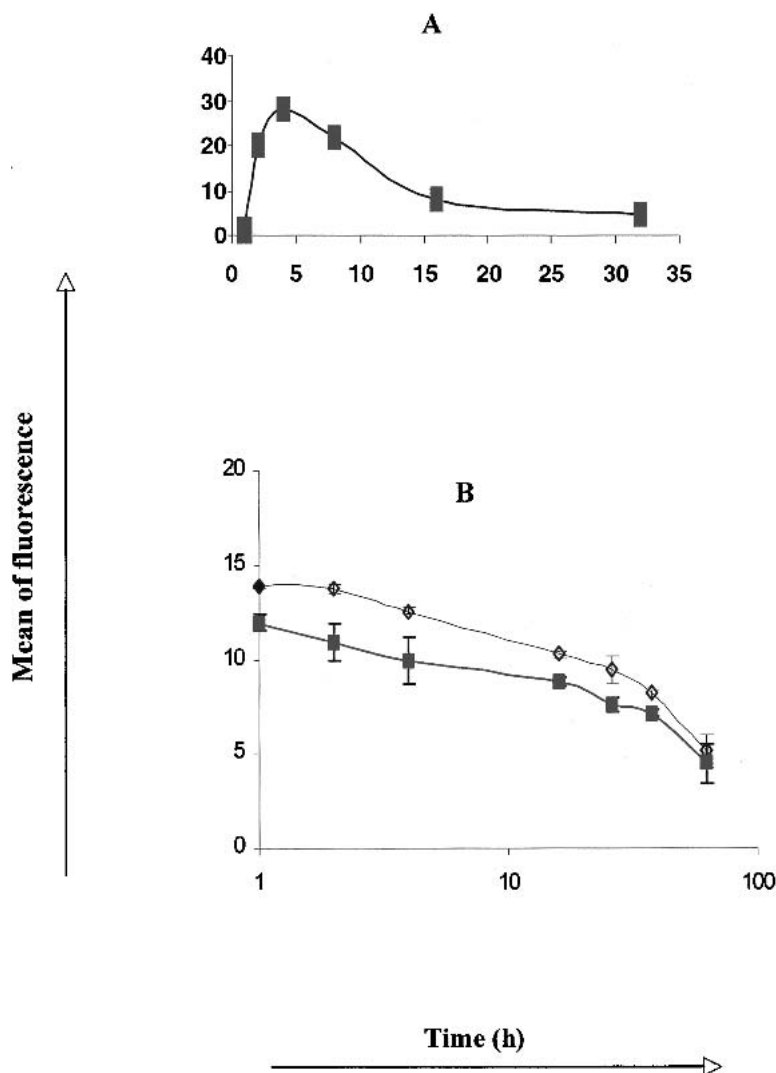


Fig. 7. Kinetics of the biologic effects and cellular retention of peptide-oligonucleotide conjugates. (A) Cells were incubated with 0.25 μ M Tat-18 (squares) or Ant-18 (diamonds) for 6 h in serum-free medium. The medium was then replaced with medium containing 10% serum and no conjugates. The cells were harvested at various times and analyzed for Luciferase activity. Data represent the means and standard errors of triplicate determinations. (B) Cells were incubated with 0.25 μ M Tat-18 (squares) or Ant-18 (diamonds) for 6 h in serum-free medium. The cells were then washed and placed in medium containing 10% serum. Total cell associated fluorescence was monitored as a function of time via flow cytometry.

nucleotide target. Additional plasmon resonance studies were performed with immobilized target oligonucleotides containing the complementary sequence embedded in different lengths of flanking oligonucleotides. The motivation for these studies was the idea that the peptide portion of the conjugate might interact with regions of the target adjacent to the region of complementarity. However, the presence of these flanking sequences had little effect on the binding

process (not shown). Thus, most of the interaction of the peptide-oligonucleotide conjugates with the target nucleic acid takes place via base pairing with the complementary sequence.

DISCUSSION

Efficient delivery of oligonucleotides to their RNA targets in the cytoplasm and nucleus remains an important issue for antisense pharmacology. A variety of lipid and polymeric carrier moieties have been found to enhance the cellular uptake of oligonucleotides. However, most of these agents only work in the cell culture setting and are unlikely to be useful *in vivo*. In many cases the effectiveness of the delivery agent is impaired by the presence of plasma proteins. In

Table II.

Name	Sequence
BIA 18	5' Biotin-TGT - AAC - TGA - GGT - AAG - AGG-3'
Random 18	5' Biotin-AGT - CAT - TTT - ATG - GCT - AAC-3'

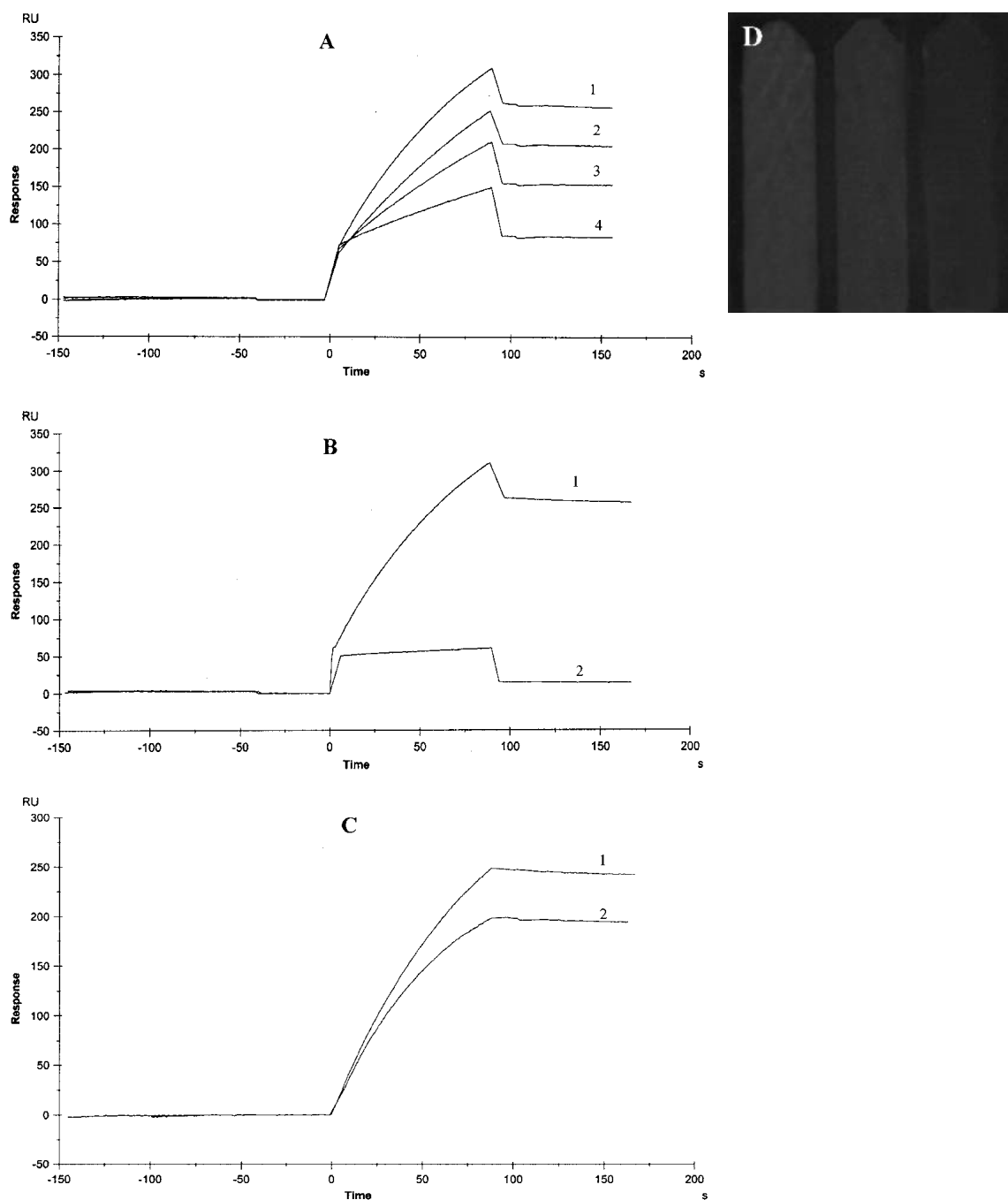


Fig. 8. Plasmon resonance analysis of the binding of peptide-oligonucleotide conjugates to their target sequences. (A) Various concentrations of Tat-18 conjugate were allowed to bind to its fully complementary oligonucleotide immobilized on sensogram chips: 1, 5 $\mu\text{g}/\text{mL}$; 2, 2.5 $\mu\text{g}/\text{mL}$; 3, 1 $\mu\text{g}/\text{mL}$; 4, 0.5 $\mu\text{g}/\text{mL}$. (B) The binding of Tat-18 (5 $\mu\text{g}/\text{mL}$) to its fully complementary oligonucleotide target (1) was compared to its binding to a target with five mismatches (2). (C) The binding of the Tat-18 (5 $\mu\text{g}/\text{mL}$) to its fully complementary oligonucleotide target (1) was compared to the binding of the 18-mer oligonucleotide alone (5 $\mu\text{g}/\text{mL}$) (no peptide conjugation) to the same target (2). (D) Fluorescence microscopy view of a sensogram chip with immobilized conjugates: left column, DNA/Tat-18 conjugate- fully complementary duplex; middle column, DNA/18-OH fully complementary duplex; right column, DNA/Tat-18 mismatch conjugate-5 mismatches duplex.

other cases, the complexes that formed between the oligonucleotide and the carrier are so large as to preclude effective *in vivo* utilization because these particles would be rapidly cleared by the phagocytes that are abundant in liver and spleen (8).

The use of cell-penetrating peptides as a delivery system for oligonucleotides may have some important advantages

over other technologies. Thus, as described here, the Tat and Ant peptide-oligonucleotide conjugates were readily taken up by cells, and significant antisense effects were achieved. The presence of serum proteins did not affect the uptake process, nor the biologic response, in agreement with results reported elsewhere (13,20). Indeed, the peptide-oligonucleotide conjugates seemed to function similarly, in terms of Luciferase

Table III.

Name	TAT 18	18-OH
kd	$5.83 \times 10^{-4} \text{ (s}^{-1}\text{)}$	$6.81 \times 10^{-4} \text{ (s}^{-1}\text{)}$
ka	$93.1 \text{ (mM}^{-1}\text{s}^{-1}\text{)}$	$74.8 \text{ (mM}^{-1}\text{s}^{-1}\text{)}$
KD	$0.626 \times 10^{-8} \text{ (M)}$	$0.91 \times 10^{-8} \text{ (M)}$
X2	0.986	0.748
Residuals	± 2	± 2

induction in the splice correction assay, in the presence of serum proteins or in their absence. In the concentration range used in this study, the peptide oligonucleotide conjugates displayed very little cytotoxicity; this would clearly be advantageous in therapeutic applications. Another potential advantage of the peptide-oligonucleotide conjugates over other oligonucleotide delivery systems is that fact that the conjugates are of moderate (~8000 daltons) molecular size. Thus they may be able to distribute broadly in the extracellular space subsequent to *in vivo* administration, as is true of unconjugated oligonucleotides (8). As a cautionary note, however, very little work has been done on the biodistribution of peptide-oligonucleotide conjugates, and interactions of the cationic moiety with plasma proteins and/or cells might be anticipated.

The total uptake and maximal biologic effect (here Luciferase induction) attainable by sub-micromolar amounts of peptide-oligonucleotide conjugate was found to be less than that achieved by complexation of similar amounts of oligonucleotides with cationic lipids. However, the potential advantages of the conjugates may not be fully revealed in short term assays of the type used here. Their modest toxicity, and their effectiveness in the presence of serum, may allow use of the conjugates during more protracted exposures with multiple dosing, potentially attaining greater effects in the long run.

An important issue explored in this report concerns the binding specificity of peptide-oligonucleotide conjugates. Potentially the presence of the cationic peptide could lessen the specificity of the antisense oligonucleotide's interaction with its target. In theory, the peptide segment could bind to the target sequence or to flanking regions via charge-charge interactions, thus compromising the specificity provided by base pairing. However, this seems not to be the case. Direct physical measurements of binding using surface plasmon resonance detected only a modest contribution of the peptide to the binding affinity of the conjugate for its nucleic acid target. Furthermore, the very sensitive biologic assay used, correction of splicing and Luciferase induction, also revealed a great deal of selectivity, with the peptide-antisense oligonucleotide conjugates showing good activity while the peptide-mismatch oligonucleotide conjugates did not. Given the fact that conjugation with the peptide does not interfere significantly with the base pairing characteristics of the oligonucleotide, the biologic action of the peptide-oligonucleotide conjugates seen here could be due equally well to effects of the intact conjugate, or to effects of "free" oligonucleotide released after intracytoplasmic reduction of the S-S linkage.

In summary, conjugates of antisense oligonucleotides with cationic cell-penetrating peptides provide a useful approach to the intracellular delivery of antisense compounds.

The presence of the peptide seems neither to enhance nor diminish the binding of the oligonucleotide to its complementary sequence, and thus specificity is maintained. The combination of a straightforward method for chemical synthesis, significant and specific biologic effects, and the potential for desirable biodistribution, suggest that the peptide-oligonucleotide conjugate approach may have considerable promise for enhancing the pharmacological applications of antisense oligonucleotides.

ACKNOWLEDGMENTS

This work was supported by NIH Grant PO1 GM59299 to RLJ. The authors thank Dr. R. Kole for his advice and Brenda Asam for outstanding editorial assistance.

REFERENCES

1. C. F. Bennett. Antisense oligonucleotides: Is the glass half full or half empty? *Biochem. Pharmacol.* **55**:9-19 (1998).
2. C. A. Stein and Y.-C. Cheng. Antisense oligonucleotides as therapeutic agents - is the bullet really magical? *Science* **261**:1004-1012 (1993).
3. P. Wittung-Stafshede. Genetic medicine - when will it come to the drugstore. *Science* **281**:657-658 (1998).
4. P. T. Ho and D. R. Parkinson. Antisense oligonucleotides as therapeutics for malignant diseases. *Semin. Oncol.* **24**:187-202 (1997).
5. J. S. Waters, A. Webb, D. Cunningham, P. A. Clarke, F. Raynaud, F. di Stefano, and F. E. Cotter. Phase I clinical and pharmacokinetic study of bcl-2 antisense oligonucleotide therapy in patients with non-Hodgkin's lymphoma. *J. Clin. Oncol.* **18**:1812-1823 (2000).
6. S. T. Croke. Molecular mechanisms of action of antisense drugs. *Biochim. Biophys. Acta* **1489**:31-44 (1999).
7. A. M. Gewirtz, D. L. Sokol, and M. Z. Ratajczak. Nucleic acid therapeutics: state of the art future prospects. *Blood* **92**:712-736 (1998).
8. R. L. Juliano, S. Alahari, H. Yoo, R. Kole, and M. Cho. Antisense pharmacodynamics: critical issues in the transport and delivery of antisense oligonucleotides. *Pharm. Res.* **16**:494-502 (1999).
9. J. G. Lewis, K.-Y. Lin, A. Kothavale, W. M. Flanagan, M. D. Matteucci, R. B. DePrinc, R. A. J. Mook, R. W. Hendren, and R. W. Wagner. A serum-resistant cytofectin for cellular delivery of antisense oligodeoxynucleotides and plasmid DNA. *Proc. Natl. Acad. Sci. USA* **93**:3176-3181 (1996).
10. P. L. Felgner, Y. J. Tsai, L. Sukhu, C. J. Wheeler, M. Manthorpe, J. Marshall, and S. H. Cheng. Improved cationic lipid formulations for *in vivo* gene therapy. *Ann. N.Y. Acad. Sci.* **772**:126-139 (1995).
11. R. DeLong, K. Stephenson, T. Loftus, S. K. Alahari, M. H. Fisher, and R. L. Juliano. Characterization of complexes of oligonucleotides with polyamidoamine starburst dendrimers and effects on intracellular delivery. *J. Pharm. Sci.* **86**:762-764 (1997).
12. H. Yoo, P. Sazani, and R. L. Juliano. PAMAM dendrimers as delivery agents for antisense oligonucleotides. *Pharm. Res.* **16**:1799-1804 (1999).
13. M. Lindgren, M. Hallbrink, A. Prochiantz, and U. Langel. Cell-penetrating peptides. *Trends Pharm. Sci.* **21**:99-103 (2000).
14. R. L. Juliano and H. Yoo. Aspects of the transport and delivery of antisense oligonucleotides. *Curr. Opin. Mol. Ther.* **2**:297-303 (2000).
15. S. Falwell, J. Seery, Y. Daikh, C. Moore, L. L. Chen, B. Pepinsky, and J. Barsboom. Tat mediated delivery of heterologous proteins into cells. *Proc. Natl. Acad. Sci. USA* **91**:664-668 (1994).
16. D. Derossi, S. Calvet, A. Trembleau, A. Brunissen, G. Chassaing, and A. Prochiantz. Cell internalization of the third helix of the Antennapedia homeodomain is receptor-independent. *J. Biol. Chem.* **271**:18188-18193 (1996).
17. E. Vives, P. Brodin, and B. Lebleu. A truncated HIV-1 Tat protein basic domain rapidly translocates through the plasma mem-

- brane and accumulates in the cell nucleus. *J. Biol. Chem.* **272**:16010–16017 (1997).
18. G. Aldrian-Herrada, M. G. Desarmenien, H. Orcel, L. Boissin-Agasse, J. Mery, J. Brugidou, and A. Rabie. A peptide nucleic acid (PNA) is more rapidly internalized in cultured neurons when coupled to a retro-inverso delivery peptide. The antisense activity depresses the target mRNA and protein in magnocellular oxytocin neurons. *Nucleic Acids Res.* **26**:4910–4916 (1998).
 19. M. Pooga, U. Soomets, M. Hallbrink, A. Valkna, K. Saar, K. Rezaei, U. Kahl, J. X. Hau, X. J. Xu, Z. Wiesenfeld-Hallin, T. Hokfelt, T. Bartfai, and U. Langel. Cell penetrating PNA constructs regulate galanin receptor levels and modify pain transmission in vivo. *Nat. Biotechnol.* **16**:857–861 (1998).
 20. A. Astriab-Fisher, D. S. Sergueev, M. Fisher, B. R. Shaw, and R. L. Juliano. Antisense inhibition of P-glycoprotein expression using peptide-oligonucleotide conjugates. *Biochem. Pharmacol.* **60**:83–90 (2000).
 21. H. Nagahara, A. M. Vocero-Akbani, E. L. Snyder, A. Ho, D. G. Latham, N. A. Lissy, M. Becker-Hapak, S. A. Ezhevshy, and S. F. Dowdy. Transduction of full-length TAT fusion proteins into mammalian cells: TAT-p27Kip1 induces cell migration. *Nat. Med.* **4**:1449–1452 (1998).
 22. S. R. Schwarze, A. Ho, A. Vocero-Akbani, and S. F. Dowdy. In vivo protein transduction: delivery of a biologically active protein into the mouse. *Science* **285**:1569–1572 (1999).
 23. R. Kole. Modification of pre-mRNA splicing by antisense oligonucleotides. In C. A. Stein and A. M. Krieg (eds.), *Applied Antisense Oligonucleotide Technology*, Wiley-Liss, Inc., New York, 1998 pp. 451–469.
 24. H. Sierakowska, M. J. Sambade, S. Agrawal, and R. Kole. Repair of thalassemic human beta-globin mRNA in mammalian cells by antisense oligonucleotides. *Proc. Natl. Acad. Sci. USA* **93**:12840–12844 (1996).
 25. G. Lacerra, H. Sierakowska, C. Carestia, S. Fucharoen, J. Summerton, D. Weller, and R. Kole. Restoration of hemoglobin A synthesis in erythroid cells from peripheral blood of thalassemic patients. *Proc. Natl. Acad. Sci. USA* **97**:9591–9596 (2000).
 26. S. H. Kang, M. J. Cho, and R. Kole. Up-regulation of the luciferase gene expression with antisense oligonucleotides: implications and applications in functional assay development. *Biochemistry* **37**:6235–6239 (1998).
 27. E. Vives and B. Lebleu. Selective coupling of a highly basic peptide to an oligonucleotide. *Tetrahedron Lett.* **38**:1183–1186 (1997).
 28. U. Jonsson et al. Real-time biospecific interaction analysis using surface plasmon resonance and a sensor chip technology. *Bio-techniques* **11**:620–627 (1991).